

RSC Advances



This is an *Accepted Manuscript*, which has been through the Royal Society of Chemistry peer review process and has been accepted for publication.

Accepted Manuscripts are published online shortly after acceptance, before technical editing, formatting and proof reading. Using this free service, authors can make their results available to the community, in citable form, before we publish the edited article. This *Accepted Manuscript* will be replaced by the edited, formatted and paginated article as soon as this is available.

You can find more information about *Accepted Manuscripts* in the [Information for Authors](#).

Please note that technical editing may introduce minor changes to the text and/or graphics, which may alter content. The journal's standard [Terms & Conditions](#) and the [Ethical guidelines](#) still apply. In no event shall the Royal Society of Chemistry be held responsible for any errors or omissions in this *Accepted Manuscript* or any consequences arising from the use of any information it contains.

Real-time Selective Monitoring of Allergenic *Aspergillus* Molds using Pentameric Antibody-Immobilized Single-Walled Carbon Nanotube-Field Effect Transistors

Joon-Hyung Jin,^a Junhyup Kim,^a Taejin Jeon,^a Su-Kyoung Shin,^b Jong-Ryeul Sohn,^c Hana Yi,^b and Byung Yang Lee*^a

^a*Department of Mechanical Engineering, Korea University, 145, Anam-ro, Seoungbuk-gu, Seoul 136-713, Korea*

^b*Department of Public Health Science, Graduate School, Korea University, 139, Bogukmun-ro, Seongbuk-gu, Seoul 136-703, Korea*

^c*Department of Environmental Health, Korea University, 139, Bogukmun-ro, Seongbuk-gu, Seoul 136-703, Korea*

E-mail: blee@korea.ac.kr

Abstract

Airborne fungus, including *Aspergillus* species, is one of the major causes of human asthma. Conventional immunoassay or DNA-sequencing techniques, although widely used, are usually labor-intensive, time-consuming and expensive. In this paper, we demonstrate a sensor for the rapid detection of *Aspergillus niger*, a well-known allergenic fungal species, using single-walled carbon nanotube (SWNT) field effect transistors (FETs) functionalized with pentameric antibodies that specifically bind to *Aspergillus* species. This strategy resulted in real time and highly sensitive and selective detection of *Aspergillus* due to electrostatic gating effect from the *Aspergillus* fungus. This mechanism is in contrast to previously reported *Aspergillus* sensor, which was based on mobility modulation from *Aspergillus* adsorption. Also, our sensor shows much wider detection range from 0.5 pg mL⁻¹ and 10 µg mL⁻¹ with a lower detection limit of 0.3 pg mL⁻¹. The resulting SWNT-FET was able to selectively detect *Aspergillus* molds in the presence of more concentrated amounts of other mold species such as *Alternaria alternata*, *Cladosporium cladosporioides*, and *Penicillium chrysogenum*. We expect that our results can be used in real-time monitoring the indoor air quality of a variety of public facilities for the elderly and children, who are more vulnerable to environmental biohazards.

Keywords: *Aspergillus*, EDC/NHS, field-effect transistor, FITC-labeled antibody, pentameric antibody immobilization, single-walled carbon nanotubes

Introduction

Allergen causes an immunoglobulin E-involved abnormal immune response known as type I hypersensitivity reaction.¹ Allergens are widely spread in a variety of different forms such as volatile organic chemicals, fine dust particles, pollens, virus, fungi, and even foods.²⁻⁴ Among fungal allergens, the *Aspergillus*, *Alternaria*, *Cladosporium*, and *Penicillium* species are the most frequently observed fungal allergens, and most of them produce allergens from their hyphae even before spore germination.⁵ Although fungi occupy a great portion of officially-recognized allergenic disorders approved by the World Health Organization and International Union of Immunological Societies, and about 19 % of patients suffering from respiratory allergic disorders including asthma are allegedly susceptible to the fungal allergens, the working mechanism of allergenic disorder is not fully understood, and no early warning systems for monitoring fungal allergens have been developed.¹ In addition, conventional fungi detection methods usually involve sampling of fungal spores and culturing for signal amplification, followed by immunoassays for optical detection, DNA sequencing, and spectroscopic quantification, which are labor-intensive, time-consuming, and costly.⁶⁻⁹ Sensors based on nanostructured materials combined with highly selective biological receptors have been reported, sometimes showing sub-picomolar detection.¹⁰ A carbon nanotube-based sensor has actually been introduced for monitoring specific peptide strands and *Aspergillus* molds.^{11, 12} Also, a cantilever array sensor has been demonstrated to monitor the growth of *Aspergillus niger* (*A. niger*).¹³ However, these previous attempts commonly employed mediator proteins for the correct orientation of the immobilized antibodies. Although nanotube and nanowire-based field-effect transistors have been widely investigated and showed excellent achievements in gas sensing and biosensing applications,^{11, 12, 14-16} such an indirect combination of antibodies with the underneath nanotube requires a more complicated fabrication procedure and accordingly causes a bigger sensor-to-sensor variation that may restrict dynamic detection range of the nanotube-based sensors.

Here, we demonstrate a nanoscale sensor for the real-time detection of *A. niger* with high sensitivity and selectivity by directly combining single-walled carbon nanotube-integrated field effect transistors (SWNT-FETs) with mouse anti-*Aspergillus* species-specific primary antibodies (WF-AF-1 Abs), which belong to an immunoglobulin M (IgM) class that can be found mostly in pentamer and sometimes in hexamer structures composed of five or six unit

antibodies. This IgM antibody selectively binds to galactomannan, a major cell wall component of *Aspergillus* species.¹⁷⁻²⁰ The activity of the WF-AF-1 Abs was carefully determined using enzyme-linked immunosorbent assay (ELISA) in various temperature conditions. The antibody was then covalently immobilized on the SWNT channel using EDC/NHS chemistry.²¹⁻²³ Continuous current increase of the SWNT-FET was observed with increasing fungal concentration, which is in contrast to previously reported method using antibodies with mediator proteins.^{11, 12} Furthermore, the detection limit was three orders lower, and the dynamic range was one hundred thousand times wider than previous report.¹² We propose that this performance difference is primarily due to the use of structurally more robust IgM antibodies combined with increased Debye length by using low ionic concentration buffer solution.

Experimental section

Reagents

1-Ethyl-3-(3-dimethylaminopropyl)-carbodiimide (EDC) and *N*-Hydroxysuccinimide (NHS) for the activation of carboxylic acid groups of SWNTs were purchased from Aldrich (Milwaukee, USA). WF-AF-1 Abs (MCA 2576, AbD Serotec) for the functionalization of the SWNT channels and fluorescein isothiocyanate (FITC, LNK061F, AbD Serotec) for labelling the WF-AF-1 Abs were purchased from Bio-Rad Laboratories, Inc. A 0.2% (v/v) octadecyltrichlorosilane (OTS) (> 90%, Aldrich Chemical Co., Inc.) solution in *n*-hexane (anhydrous 95%, Aldrich Chemical Co., Inc.) was prepared for aligning and patterning the SWNT channels.

Equipment

Atomic force microscopy (AFM) and scanning electron microscopy (SEM) images were obtained using NTEGRA Prima (TS-150, NT-MDT) and S-4300N (Hitachi High-Technologies Corp.), respectively. The effect of the applied gate voltage, both in air and liquid, was monitored using a probe station equipped with a Keithley 4200 semiconductor parameter analyzer. A wired Pt tip was used as a pseudo-reference electrode. I-V

characteristics of the SWNT-FETs were recorded using a potentiostat/galvanostat (Reference 600, Gamry Instruments).

SWNT-FET fabrication

A boron-doped p-Si wafer with 300 nm thick thermal oxide (SiO_2) was used (resistivity = 1.0–10.0 $\Omega\cdot\text{cm}$). Electrode pads consisting of 30 nm-thick Au film over 5 nm-thick Cr adhesion layer was formed via photolithography using photoresist (AZ5214) followed by thermal evaporation of metals and lift-off process. Regions of non-polar OTS and SiO_2 were patterned between the electrode pads. The OTS patterned substrate was dipped into SWNT (Hanwha Chemical Co., Ltd.) solution to form a SWNT network channel. The SWNTs assembled on the SiO_2 regions, avoiding the OTS regions. Additional Cr/Au deposition right on the junction area between the SWNT and the Au electrode allowed better mechanical strength and reduced contact resistance. The final step was to immobilize the *Aspergillus* species-specific receptors WF-AF-1 Abs on the SWNTs. The entire fabrication processes are shown in Scheme 1. Thirty eight devices were available from a 4" p-Si wafer, and each device had two SWNT-FET channels.

Direct immobilization of mouse anti *Aspergillus* species-specific primary antibodies WF-AF-1 Abs

Acid treatment of SWNTs after their growth for catalytic particle removal inevitably overoxidizes backbone carbons of the SWNTs to form many oxygen-containing chemical functional groups such as carboxylic acid groups on the SWNT surface.²⁴ Although the carboxylic acid groups are reactive with amine groups, the amide forming reaction, under normal conditions, could be kinetically unfavorable without a catalyst. As shown in Scheme 1, the EDC/NHS chemistry substitutes the hydroxyl group of the carboxylic acid group with more facile leaving group, i.e., NHS group. Afterwards, the nucleophilic attack of the *N*-terminal of an antibody on the succinimide-substituted carbonyl carbon was enhanced and formed a strong amide bond. The resulting antibody-immobilized SWNT-FET devices were stored at 4 °C before use.

Strains and growth conditions

The fungal strains used in this study were obtained from the RDA Genebank Information Center of Korea. *A. niger* KACC 40280, *Alternaria alternata* (*A. alternata*) KACC 43544, *Cladosporium cladosporioides* (*C. cladosporioides*) KACC 43384, and *Penicillium chrysogenum* (*P. chrysogenum*) KACC 44307 were grown at 25 °C for 6 days in malt extract agar. Fungal fragments and spores were harvested with sterile loops and washed twice in phosphate-buffered saline (PBS, pH7.2). They were resuspended to 1.2×10^7 spores mL⁻¹ (5.7 mg mL⁻¹ in wet weight) in 50 mM carbonate bicarbonate buffer (pH 9.6, Sigma) and ten-fold dilution series of the suspensions were prepared. The fungal concentration was determined by hemocytometer.

Enzyme-linked immunosorbent assay

Indirect ELISA was carried out by coating 200 µL aliquots of different concentrations of *A. niger* samples in 50 mM carbonate bicarbonate buffer to each well of microplates (NUNC Maxisorp, Nalgene). The plates were incubated overnight at 4 °C, then washed twice with 200 µL PBS buffer with 0.05% Tween-20 (PBST). 200 µL of WF-AF-1 Abs in PBS buffer with 1% BSA (1.0 mg/ml, 1:1000) was added and the plates were incubated at different temperatures (7, 25, and 37 °C) for two hours. After washing the plates twice with 200 µL PBS, 200 µL HRP conjugated goat-anti-mouse Abs (Bio-Rad) in 1% BSA/PBS (1.0 mg mL⁻¹, 1:1000) was then applied to each well and incubated at various temperatures (7, 25, and 37 °C) for one hour. After washing the plates twice with 200 µL PBST, 100 µL peroxidase substrate (Bio-Rad Laboratories) was added to each well and the plates were incubated for 10 min at room temperature for the blue-green color development. The enzyme reaction was stopped by adding 2% oxalic acid (Sigma-Aldrich). The optical density at 415 nm was read using a microplate reader Victor™ X3 (Perkin Elmer Inc., USA). Fig. 1 shows that more than 70 % of the antibodies are still active at 7 °C as compared to that at a higher temperature up to 37 °C, indicating excellent stability of WF-AF-1 Abs at a wide range of temperature.

Fungal cell counting and weighing

To quantify molds, we directly count the fungal spores using hemocytometer and an optical microscope (Eclipse LV100ND, Nikon). Fig. S1 presents the microscope image showing suspended mold spores in buffer solution. We can define the mold spores per unit volume of the mold-suspended solution because grid distance and the well depth of the hemocytometer

are given values. However, mass quantity is a more convenient mold quantification method for our experiment since WF-AF-1 Abs binds to both spores and fragments of *A. niger*. Fungal fragments are prevalently present in biosphere including air and water.²⁵⁻²⁷ Averaged mass for a spore of *A. niger* is known as 47 pg.²⁸ To measure such a small mass, a PCR tube container was placed on the weighing plate of an ultra microbalance (XF2U, Mettler Toledo), and as shown in Fig. S2 three more containers which include silica gels were placed in the weighing chamber to protect hygroscopic fungal spores and fragments from moisture. Actual mass of mold could be obtained simply by subtracting the mass of PCR tube container from total mass. Fresh molds grown on agar plates were used to measure the mass. The molds were finally suspended in a PBS solution and diluted to a concentration of 100 $\mu\text{g mL}^{-1}$.

Simulated clinical test and reversibility experiment

For the mixture experiment in Fig. 5e, we first prepared a primary antibody-immobilized SWNT-FET sensor, and then we first injected 2 μL PBS buffer and waited for current stabilization. Afterwards, we sequentially injected, in 50 sec intervals, 2 μL of the four mixtures prepared as follows: 1:1 (v/v) mixture of 10 $\mu\text{g mL}^{-1}$ *C. cladosporioides* and 10 $\mu\text{g mL}^{-1}$ *A. alternata*; 1:1:1 (v/v) mixture of 10 $\mu\text{g mL}^{-1}$ *C. cladosporioides*, 10 $\mu\text{g mL}^{-1}$ *A. alternata*, and 10 $\mu\text{g mL}^{-1}$ *P. chrysogenum*; 1:1:1:1 (v/v) mixture of 10 $\mu\text{g mL}^{-1}$ *C. cladosporioides*, 10 $\mu\text{g mL}^{-1}$ *A. alternata*, 10 $\mu\text{g mL}^{-1}$ *P. chrysogenum*, and 1 $\mu\text{g mL}^{-1}$ *A. niger*; 1:1:1:1 (v/v) mixture of 10 $\mu\text{g mL}^{-1}$ *C. cladosporioides*, 10 $\mu\text{g mL}^{-1}$ *A. alternata*, 10 $\mu\text{g mL}^{-1}$ *P. chrysogenum*, and 10 $\mu\text{g mL}^{-1}$ *A. niger*. Note that the first two mixtures contain no *A. niger*. The last two mixtures contain *A. niger* of concentrations differing by 10 times. For the reversibility experiment in Fig. 5f, we first prepared a primary antibody-immobilized SWNT-FET sensor, and then we first injected 2 μL PBS buffer and waited for current stabilization. Then, we injected 2 μL of 1 pg mL^{-1} *A. niger* and observed the current increase. Afterwards, the current monitoring was stopped momentarily for sample washing. The sample was thoroughly washed with PBS and D.I water for 5 min. Then, the current monitoring was resumed. This process was repeated for two times.

Results and discussion

Direct immobilization of pentameric WF-AF-1 Abs on the SWNT channel

Scheme 1 describes the preparation procedure of SWNT-FET and the following immobilization of WF-AF-1 Abs on the SWNT channel. Sequential steps finally lead to the production of the *Aspergillus* sensors that have the SWNT network channel as sensor transducers.²⁹ The SWNTs in the channel selectively assembly on the SiO₂ region due to van der Waals interaction, while avoiding the nonpolar OTS regions. Subsequently, WF-AF-1 Abs were immobilized on the SWNT surfaces via EDC/NHS chemistry utilizing carboxyl acid groups on the SWNT surface that are introduced during SWNT growth and cleaning process.²⁴ Note that this immobilization scheme is advantageous compared to the previous *Aspergillus* sensor using SWNT-FET,¹² because by directly attaching the antibody to the SWNT, we can reduce the SWNT-antibody distance, and therefore enhance sensitivity.³⁰

Basic characterization of SWNT-FET

The gap between source and drain electrodes is approximately 10 μm as shown in Fig. 2a. The corresponding SEM image of the SWNT channel having a width of 5 μm proves that a well-oriented SWNT network channel was formed between source and drain. The channel could be formed simply by dipping the OTS-patterned SiO₂ substrate into a SWNT dispersed solution, and the SWNTs were selectively assembled on the exposed SiO₂ regions while avoiding the nonpolar OTS regions. The I-V curve of the SWNT-FET shown in Fig. 2b verifies the Schottky barrier junction featuring rectifying characteristics formed in both ends of the SWNT channel between the semiconducting SWNTs and the deposited gold metal.^{31,32} To verify the usability of the SWNT-FET as a sensor transducer, we measured the back gate characteristics of the SWNT-FET in air. Fig. 2c shows a typical back gate characteristic of a SWNT-FET. The oxide layer was 100 nm. The SWNT-FET showed a p-type semiconductor behavior, where the conductance decreased with the increase of gate voltage (V_g).³³ The typical on-off ratio was ~ 9 . The apparent low current on/off ratio of our sensor transducers was mainly due to the utilization of as-produced SWNTs, which are composed of mixtures of semiconducting and metallic SWNTs. The carrier mobility μ was calculated to be in the range of 5.6-8.1 $\text{cm}^2 (\text{V}\cdot\text{s})^{-1}$ (details in Supplementary Information), which is comparable to previously reported SWNT-FET-based sensors with similar on/off ratio and mobility values.^{34, 35} From the practical point of view, high resistance SWNT-FET devices were carefully screened out on the basis of resistance of the SWNT channel to minimize sensor-to-

sensor variation. Fig. 3 summarizes resistance distribution, and devices with resistances levels around several hundred k Ω were used in this experiment.

Binding and functionalization of SWNT-FET

The immobilized WF-AF-1 Abs and their binding to *A. niger* fragments were confirmed with both AFM and fluorescence microscopy (Fig 4). We prepared a solution of *A. niger* fragments by ultra-centrifugation as described in Experimental section. Then, the antibody-immobilized sensor was dipped into solution and left for \sim 1 h and then washed extensively with PBS and DI water. Fig 4a and 4b compare the SWNT channel before and after *A. niger* fragment binding. The approximate density of the channel determined by counting individual SWNT from the AFM image considering the average nanotube length of \sim 2 μ m is 5 μ m², which is well above the percolation threshold density.^{34,35} This density is known to result in similar values of current on/off ratio as our sensor transducers.³⁴ The height profile (Fig 4c) shows that the fragment binding resulted in an overall increase in the height profile by \sim 3 nm due to the fragments. The antibody WF-AF-1 Abs specifically binds to galactomannan, which is present on the surface of the spores and their fragments.²⁵⁻²⁷ This means that our sensor is sensitive to both spores and fragments of *A. niger*. We further confirmed the antibody immobilization and fragment binding by introducing FITC-conjugated WF-AF-1 Abs to the sensor (Fig. 4d). The intensive fluorescent radiation along the SWNT channel shows the successful antibody immobilization on the channel and fungal fragment binding. The actual size of spores of *Aspergillus* species is a few microns^{36,37}, which is comparable to that of the SWNT channel width (5 μ m). Accordingly, it is reasonable to say that most of the radiated emission from the channel area is due to the binding between fungal fragments and the FITC-labeled antibodies.

Sensitivity and selectivity

Current flow through the functionalized SWNT channel was recorded as a function of time with continuous injection of 2 μ L of different concentrations of *A. niger* suspended in 1.5 mM pH 7.2 PBS solution at every 50 seconds (Fig. 5a). A low concentration PBS buffer of 1.5 mM was used to increase the Debye length (\sim 9 nm around SWNTs).^{30,38,39} Since the antibody used in this work has a form of IgM, which is physically the largest antibody, Debye length is a crucial factor affecting sensing ability and selectivity. Since IgM has a planar

structure with longest diameter of ~ 30 nm and thickness of ~ 3 nm,⁴⁰⁻⁴³ we can expect many IgM antibodies to be immobilized around the SWNTs with random direction while providing multiple binding sites within the Debye length.

The amount of *A. niger* was carefully weighed using ultra-microbalance before preparing the solutions. Fig. 5b shows that the output current was linearly proportional to the *A. niger* concentration in the range from 0.5 pg mL^{-1} to $10 \text{ }\mu\text{g mL}^{-1}$ with an approximate detection limit of 0.3 pg mL^{-1} . This detection limit is three orders lower, and the dynamic range is one hundred thousand times wider than previous report.¹² The increase of current with increasing concentration can be explained from electrostatic gating effect of the *A. niger* spores and fragments. In neutral pH, the surface of *A. niger* is negatively charged because the isoelectric point of the *A. niger* is around 2.⁴⁴ The negatively charged *A. niger* spores and fragments apply a negative gating effect to the SWNT channel (Fig 2c, I- V_g curve), and therefore, the current is increased in the SWNT channel. Note that this current increase behavior is opposite to a previous report using SWNT-FET for the detection of fungi.¹² Presumably, their experiment involved mobility decrease of SWNTs by direct binding between fungi and SWNTs.⁴⁵ We checked the selectivity of our sensor by introducing successively other fungi species to the SWNT sensor. As shown in Fig. 5c, the effect on the current from injections of *A. alternata*, *C. cladosporioides*, and *P. chrysogenum*-suspended solutions are negligible as compared to that of *A. niger*-suspended solution. Observation of the selective current response of the functionalized SWNT-FET to *A. niger* can be attributed to specific binding between galactomannan on *A. niger* surface and the immobilized WF-AF-1 Abs.⁴⁶ Most cell walls of *Aspergillus* species including their conidia contain galactomannan.^{47, 48} Table S1 shows normalized current response (I_N) of the WF-AF-1 Abs-immobilized SWNT-FET device to various interfering molds. The signal output was enhanced by more than two times with the injection of *A. niger* in the presence of interfering molds. To verify the sensing mechanism, we used a Pt pseudo-reference electrode for liquid gating.^{49, 50} The I- V_{lg} shows hysteresis due to mobile ions in the liquid. Major cause for hysteresis in nanotube and nanowire-based FETs is water molecules or charge trapping at the interface between the solid substrate and nanotube/nanowires.^{15, 51, 52} Fig. 5d shows the liquid characteristics before and after the *Aspergillus* binding. The threshold voltage from the I- V_{lg} graph shifted to the right side by about 90 mV without appreciable change in slope when a 5 μL portion of interfering *A. niger* (1 pg mL^{-1}) was injected. This means the mobility was

conserved, and the increased current signal was mainly due to the increased hole carrier concentration from chemical gating by the negatively charged *A. niger* fragments. Note that our sensor has a wide dynamic range with very low detection limit compared to previous works, and the sensing mechanism is chemical gating which is predictable from the interaction between p-type SWNT-FET and negatively charged *A. niger* fragments.

The bioaerosol in real world contains many kinds of molds. To show the feasibility of using our sensor in the real-world, we prepared four different simulated clinical samples of molds and performed more detailed specificity experiments (details in Experimental section). Fig. 5e describes response of the SWNT-FET sensor to the simulated clinical samples. The sensor showed no significant response to the first two mixtures containing no *A. niger*. However, the sensor showed increasing sensor response to the last two mixtures that contain *A. niger* of concentrations differing by 10 times. To check the feasibility of using our sensors in the real world, we performed reversibility test in low target concentration (Fig. 5f). To show that the reversibility can be performed in principle, we washed the sample with extensive amount of 1mM pH 7.0 PBS buffer and D.I water (details in Experimental section). The washed sensor showed a current level close to its initial value, as shown in Fig. 5f. This shows that we can combine our sensor with additional washing system to reverse the sensor response after being exposed to target materials.

Conclusions

Here, we demonstrated a nanoscale sensor for the real-time detection of *A. niger* with high sensitivity and selectivity by directly combining single-walled carbon nanotube-integrated field effect transistors (SWNT-FETs) with mouse anti *Aspergillus* species-specific primary antibodies (WF-AF-1 Abs), which belong to an IgM class that has a form of pentamer or hexamer structure composed of five or six unit antibodies. Contrary to previous works, output current in this work increased with increased amount of the target fungal fragments due to the chemical gating effect by the antibody-allergen binding event occurring on the SWNT-FET. The utilization of structurally more robust antibody and increased Debye length due to low buffer ionic concentration appears to allow a wider detection range and lower detection limit for monitoring fungal allergens. Our study can be used to develop a new type of sensor

module for an integrated *in situ* monitoring system of fungal allergens when combined with adequate sampler that collects the airborne fungi into liquid phase.

Acknowledgments

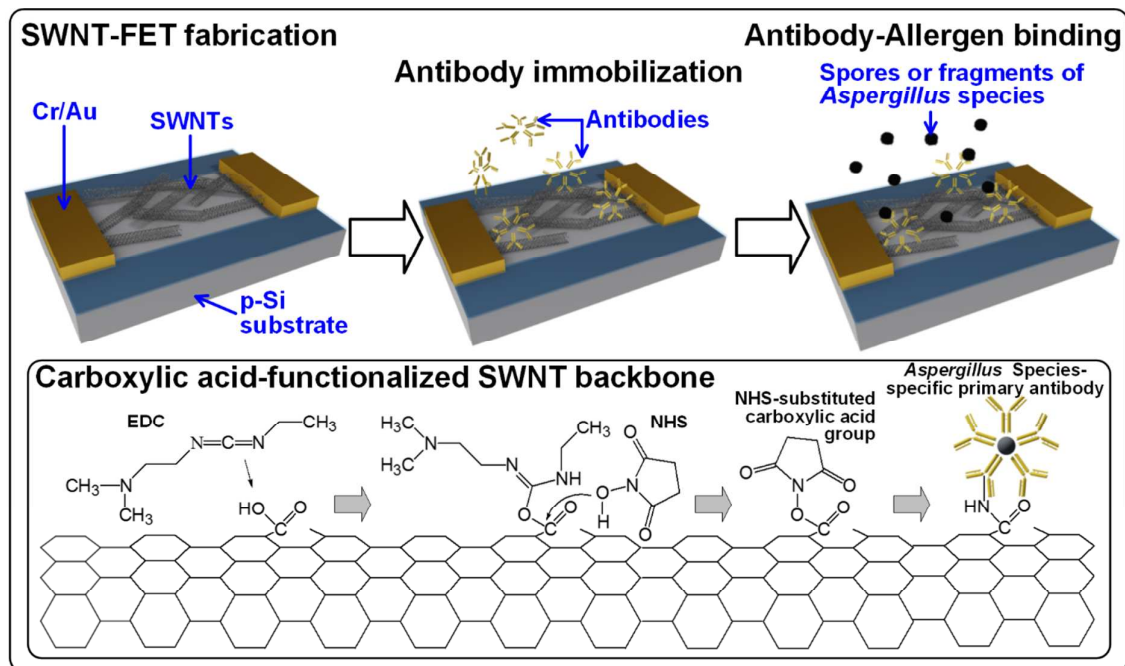
This work was supported by Korea Ministry of Environment as "The Environmental Health Action Program"(grant number: ARQ201303173002), and as "The Converting Technology Program" (grant numbers: 2013001650001 and ARQ201403075001).

References

- 1 R. Cramer, M. Garbani, C. Rhyner and C. Huitema, *Allergy*, 2014, **69**, 176.
- 2 M. Rosmilah, M. Shahnaz, G. Patel, J. Lock, D. Rahman, A. Masita and A. Noormalin, *Trop Biomed*, 2008, **25**, 243.
- 3 C. Zahradnik, R. Martzy, R. L. Mach, R. Krska, A. H. Farnleitner and K. Brunner, *Anal Bioanal Chem*, 2014.
- 4 R. J. Bertelsen, C. K. Faeste, B. Granum, E. Egaas, S. J. London, K. H. Carlsen, K. C. Lodrup Carlsen and M. Lovik, *Clin Exp Allergy*, 2014, **44**, 142.
- 5 B. J. Green, T. Z. Mitakakis and E. R. Tovey, *J Allergy Clin Immunol*, 2003, **111**, 285.
- 6 L. Monaci, R. Pilolli, E. De Angelis, M. Godula and A. Visconti, *J Chromatogr A*, 2014.
- 7 A. Pinto, P. N. Polo, O. Henry, M. C. Redondo, M. Svobodova and C. K. O'Sullivan, *Anal Bioanal Chem*, 2014, **406**, 515.
- 8 M. Koeberl, D. Clarke and A. L. Lopata, *J Proteome Res*, 2014.
- 9 M. Svobodova, T. Mairal, P. Nadal, M. C. Bermudo and C. K. O'Sullivan, *Food Chem*, 2014, **165**, 419.
- 10 S. M. Yoo, T. Kang, H. Kang, H. Lee, M. Kang, S. Y. Lee and B. Kim, *Small*, 2011, **7**, 3371.
- 11 J. Oh, G. Yoo, Y. W. Chang, H. J. Kim, J. Jose, E. Kim, J. C. Pyun and K. H. Yoo, *Biosensors & Bioelectronics*, 2013, **50**, 345.
- 12 R. A. Villamizar, A. Maroto and F. X. Rius, *Analytical and Bioanalytical Chemistry*, 2011, **399**, 119.
- 13 N. Nugaeva, K. Y. Gfeller, N. Backmann, H. P. Lang, M. Duggelin and M. Hegner, *Biosensors & Bioelectronics*, 2005, **21**, 849.
- 14 G. Konvalina and H. Haick, *Acc. Chem. Res.*, 2014, **47**, 66.
- 15 Y. Paska and H. Haick, *Acs Applied Materials & Interfaces*, 2012, **4**, 2604.
- 16 B. Wang, J. C. Cancilla, J. S. Torrecilla and H. Haick, *Nano Lett.*, 2014, **14**, 933.
- 17 P. C. Bardalaye and J. H. Nordin, *J. Biol. Chem.*, 1977, **252**, 2584.
- 18 T. Nakajima and E. Ichishima, *J. Ferment. Bioeng.*, 1994, **78**, 472.
- 19 C. M. A. Swanink, J. F. G. M. Meis, A. J. M. M. Rijs, J. P. Donnelly and P. E. Verweij, *J. Clin. Microbiol.*, 1997, **35**, 257.
- 20 Y. Tamaki, T. Teruya and M. Tako, *Biosci., Biotechnol., Biochem.*, 2010, **74**, 1110.
- 21 G. Krishnamoorthy, R. Selvakumar, T. P. Sastry, S. Sadulla, A. B. Mandal and M. Doble, *Materials Science & Engineering C-Materials for Biological Applications*, 2014, **43**, 164.
- 22 M. D'Este, D. Eglin and M. Alini, *Carbohydr. Polym.*, 2014, **108**, 239.
- 23 Y. S. Sohn and Y. K. Lee, *Journal of Biomedical Optics*, 2014, **19**.
- 24 A. Suri and K. S. Coleman, *Carbon*, 2011, **49**, 3031.
- 25 R. L. Gorny, T. Reponen, K. Willeke, D. Schmechel, E. Robine, M. Boissier and S. A. Grinshpun, *Applied and Environmental Microbiology*, 2002, **68**, 3522.
- 26 A. Pringle, *PLoS Pathog*, 2013, **9**, e1003371.
- 27 T. Reponen, S. C. Seo, F. Grimsley, T. Lee, C. Crawford and S. A. Grinshpun, *Atmos Environ (1994)*, 2007, **41**, 8140.
- 28 N. Nugaeva, K. Y. Gfeller, N. Backmann, M. Duggelin, H. P. Lang, H. J. Guntherodt and M. Hegner, *Microsc. Microanal.*, 2007, **13**, 13.
- 29 M. Lee, J. Im, B. Y. Lee, S. Myung, J. Kang, L. Huang, Y. K. Kwon and S. Hong, *Nat. Nanotechnol.*, 2006, **1**, 66.
- 30 J. P. Kim, B. Y. Lee, S. Hong and S. J. Sim, *Anal. Biochem.*, 2008, **381**, 193.
- 31 Y. He, J. Y. Zhang, S. M. Hou, Y. Wang and Z. P. Yu, *Appl. Phys. Lett.*, 2009, **94**.
- 32 S. Heinze, J. Tersoff, R. Martel, V. Derycke, J. Appenzeller and P. Avouris, *Phys. Rev. Lett.*, 2002, **89**.
- 33 M. H. Yang, K. B. K. Teo, W. I. Milne and D. G. Hasko, *Applied Physics Letters*, 2005, **87**.
- 34 V. K. Sangwan, A. Behnam, V. W. Ballarotto, M. S. Fuhrer, A. Ural and E. D. Williams, *Appl. Phys. Lett.*, 2010, **97**, 043111.
- 35 E. S. Snow, J. P. Novak, P. M. Campbell and D. Park, *Appl. Phys. Lett.*, 2003, **82**, 2145.
- 36 R. Serra, F. J. Cabanes, G. Perrone, G. Castella, A. Venancio, G. Mule and Z. Kozakiewicz, *Mycologia*, 2006, **98**, 295.
- 37 T. H. Fang, S. H. Kang, Z. H. Hong and C. D. Wu, *Micron*, 2012, **43**, 407.
- 38 J. P. Kim, B. Y. Lee, J. Lee, S. Hong and S. J. Sim, *Biosensors & Bioelectronics*, 2009, **24**, 3372.
- 39 J. Wu, K. Gerstandt, H. B. Zhang, J. Liu and B. J. Hinds, *Nat. Nanotechnol.*, 2012, **7**, 133.
- 40 E. Stern, R. Wagner, F. J. Sigworth, R. Breaker, T. M. Fahmy and M. A. Reed, *Nano Lett.*, 2007, **7**, 3405.
- 41 S. J. Armstrong, M. C. Outlaw and N. J. Dimmock, *Journal of General Virology*, 1990, **71**, 2313.
- 42 B. Chesebro, B. Bloth and S. E. Svehag, *J Exp Med*, 1968, **127**, 399.
- 43 P. W. Haebel, D. Goldstone, F. Katzen, J. Beckwith and P. Metcalf, *EMBO J.*, 2002, **21**, 4774.

- 44 P. Jones, D. Moore and A. P. J. Trinci, *J. Gen. Microbiol.*, 1988, **134**, 235.
- 45 I. Heller, A. M. Janssens, J. Männik, E. D. Minot, S. G. Lemay and C. Dekker, *Nano Lett.*, 2008, **8**, 591.
- 46 H. E. Jensen, J. Salonen and T. O. Ekfors, *J Pathol*, 1997, **181**, 100.
- 47 S. Christgau, S. Kauppinen, J. Vind, L. V. Kofod and H. Dalboge, *Biochem Mol Biol Int*, 1994, **33**, 917.
- 48 P. Ademark, R. P. de Vries, P. Hagglund, H. Stalbrand and J. Visser, *Eur J Biochem*, 2001, **268**, 2982.
- 49 I. Heller, A. M. Janssens, J. Männik, E. D. Minot, S. G. Lemay and C. Dekker, *Nano Letters*, 2007, **8**, 591.
- 50 S. Rosenblatt, Y. Yaish, J. Park, J. Gore, V. Sazonova and P. L. McEuen, *Nano Letters*, 2002, **2**, 869.
- 51 W. Kim, A. Javey, O. Vermesh, Q. Wang, Y. Li and H. Dai, *Nano Lett.*, 2003, **3**, 193.
- 52 K. Bradley, J. Cumings, A. Star, J.-C. P. Gabriel and G. Grüner, *Nano Letters*, 2003, **3**, 639.

Figures



Scheme 1 Schematic diagram depicting fabrication of the SWNT-FET-based fungi sensors and the antibody-allergen binding. Note that WF-AF-1 Abs were directly immobilized on the carboxylic acid-functionalized SWNT surface via EDC/NHS chemistry.

Figures

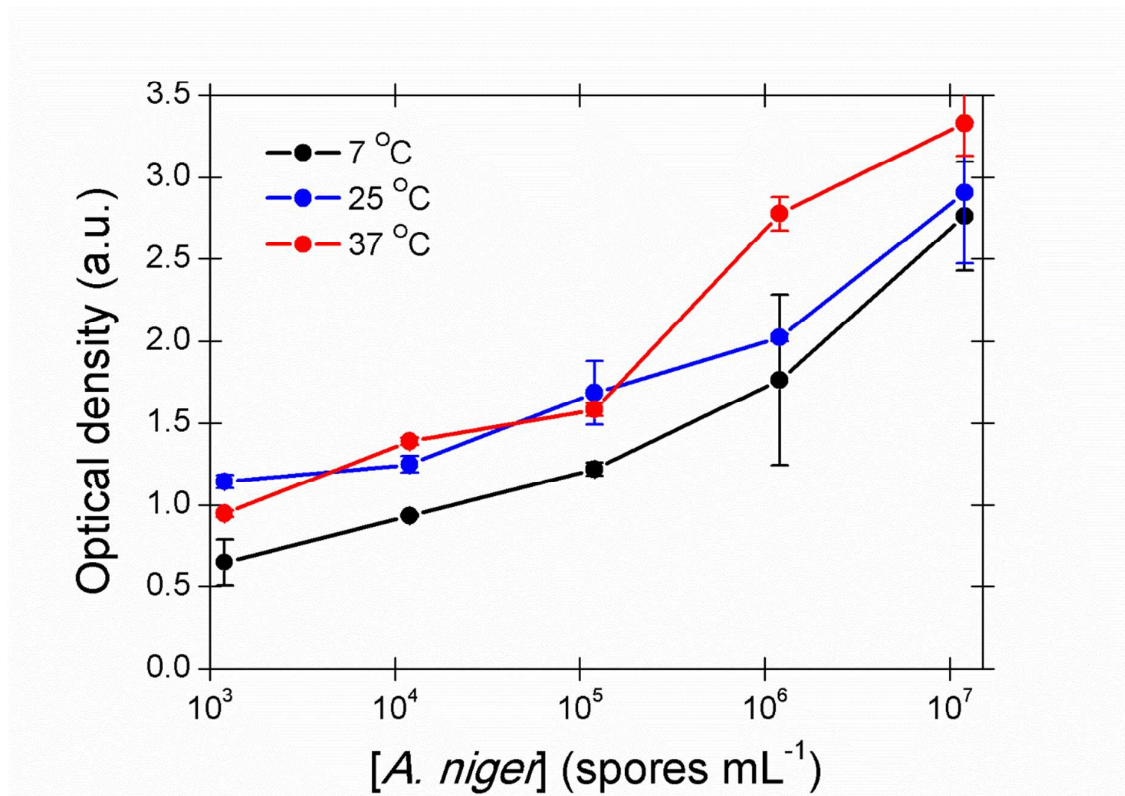


Fig. 1 ELISA optical density measurements for testing antibody activity of WF-AF-1 at 7 °C , 25 °C, and 37 °C.

Figures

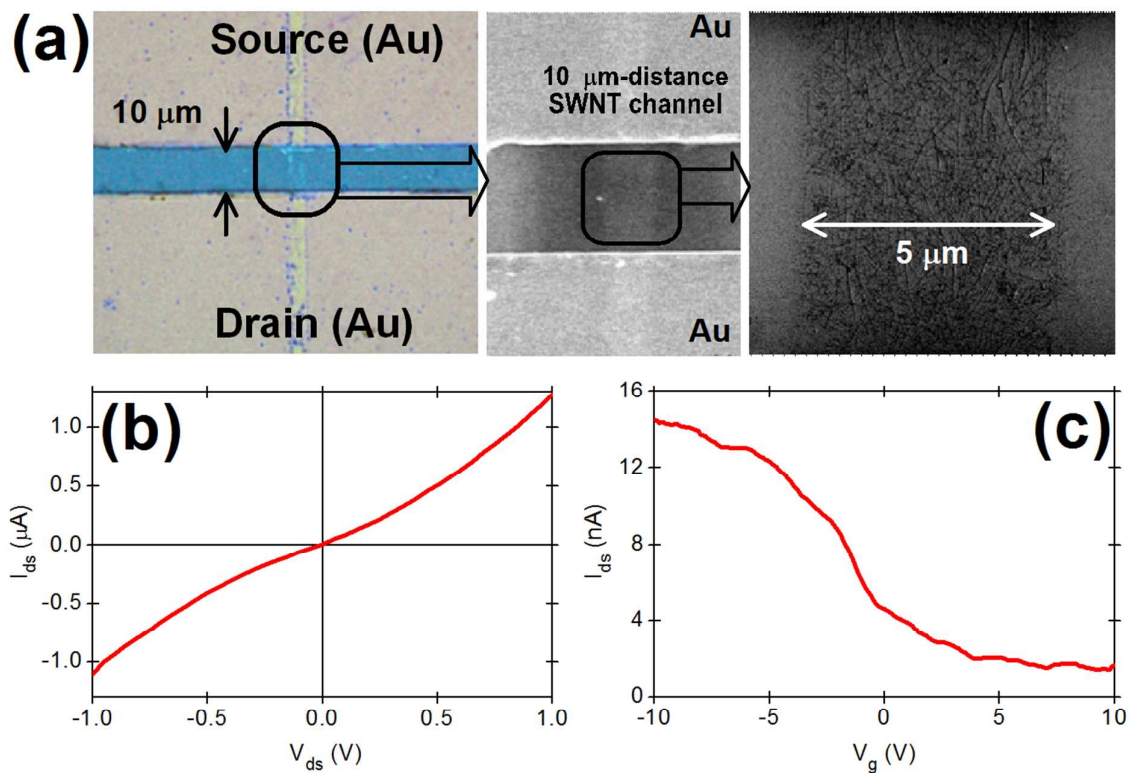


Fig. 2 Electronic properties of SWNT FETs. (a) Detailed images of the 5 μm wide, 10 μm long SWNT channel. (b) An example of the I-V characteristic curve of a device with a resistivity of 830 kΩ to confirm the Schottky-barrier junction at both Au-SWNT and SWNT/Au interfaces: scan rate = 50 mV s⁻¹. Note that the resistivity of the devices were measured with assuming linear I-V characteristics. (c) Dependence of source current on the applied gate voltage at source-drain voltage $V_{ds} = 0.1$ V.

Figures

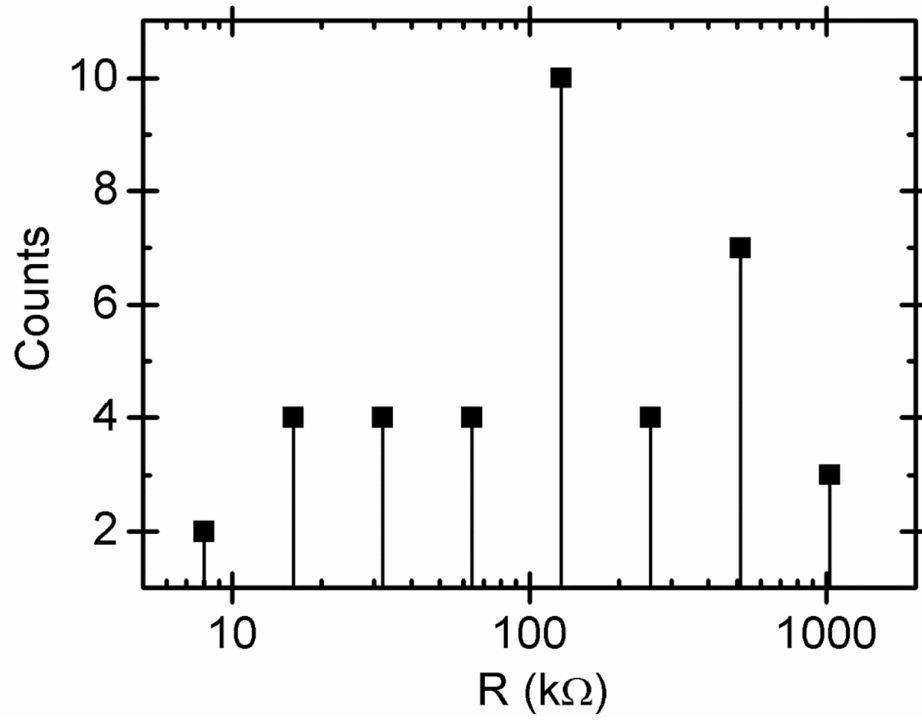


Fig. 3 Resistance distribution of the SWNT-FET devices.

Figures

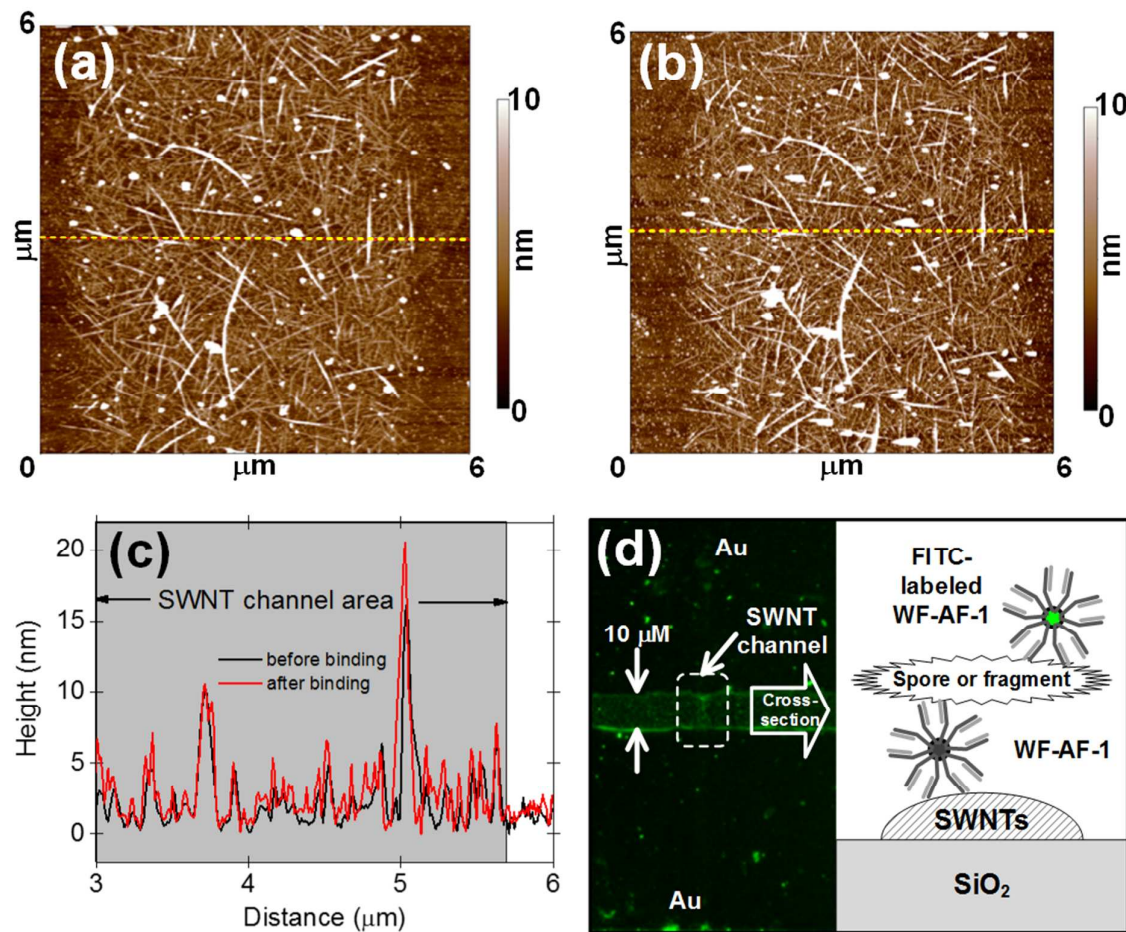


Fig. 4 Verification of antibody immobilization and fungi fragment-antibody binding. AFM images of WF-AF-1 Abs-immobilized SWNT channels (a) before and (b) after the antibody-allergen binding, and (c) corresponding height profiles. (d) Fluorescence microscopy image of FITC-labeled SWNT-FET sensor after fragment binding: excitation wavelength = 465 ~ 495 nm (Nikon eclipse LV100ND); exposure time = 60 s.

Figures

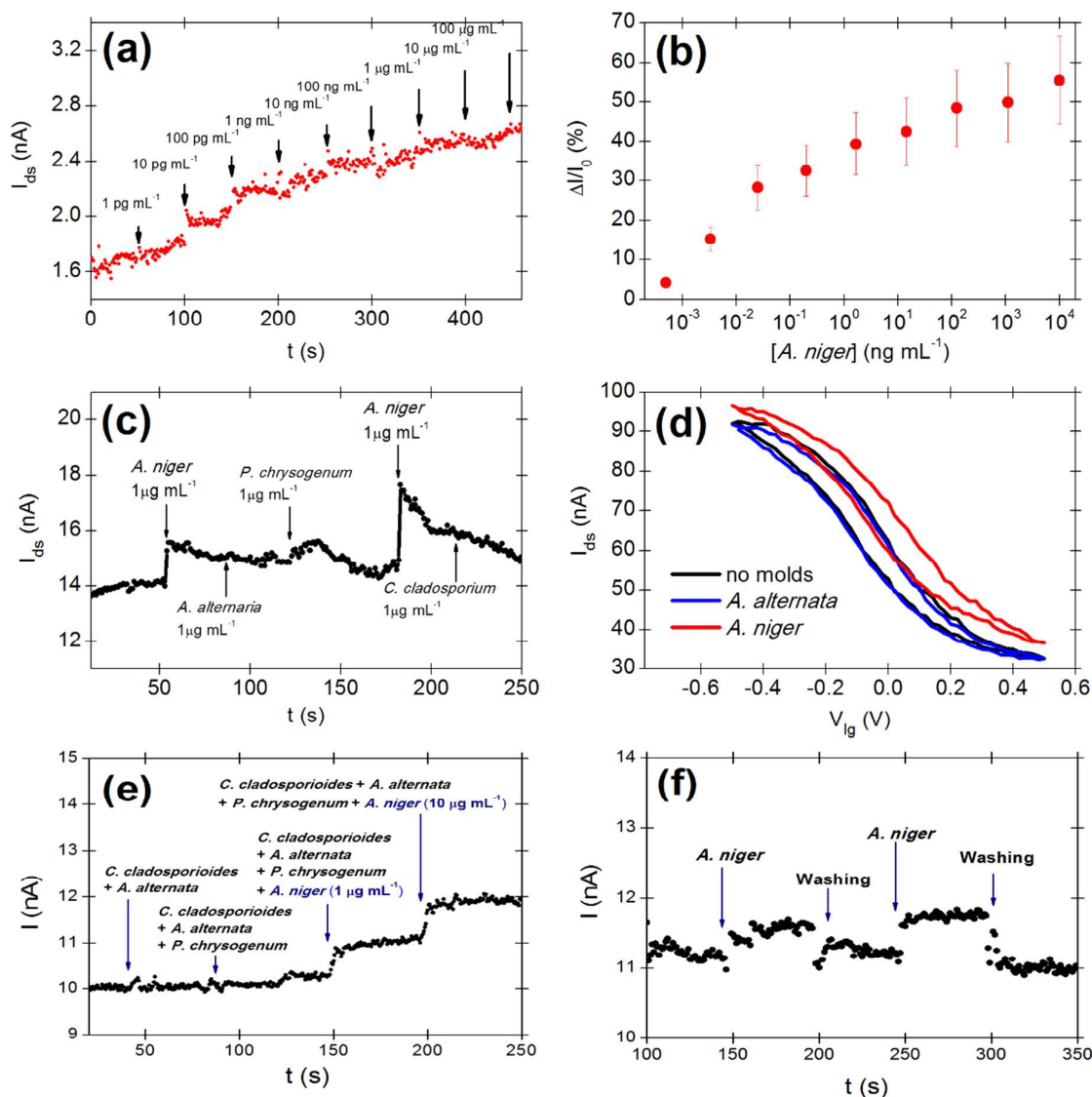


Fig. 5 Response of *A. niger* sensor. (a) Real-time response of WF-AF-1 Abs-immobilized SWNT-FET device to consecutively injected *A. niger*-suspended PBS solution in various concentrations (injection volume = 2 μL). Note that the initial volume of the 1.5 mM PBS solution on the device is 2 μL; (b) Corresponding calibration curve; (c) Real-time responses of the functionalized SWNT-FET device to sequential injections of different mold-suspended PBS solutions in random order; (d) Selective liquid gating effect of our sensor to target and non-target molds. Injection volume and concentration are the same for both *A. alternata* and *A. niger* as 5 μL and 1 pg mL⁻¹, respectively. ($V_{ds} = 0.1$ V; initial volume of 1.5 mM PBS = 10 μL); (e) Sequential injection of four different mixtures of fungal solutions. The first two mixtures contain no *A. niger*, while the last two mixtures contain *A. niger* of concentrations differing by 10 times; (f) Sensor revival test by extensive washing with PBS buffer and water.